CrossMark

Novel system for simultaneously measuring the thickness and refractive index of a transparent plate with two optical paths

Chien-Sheng Liu[1] [ORCID] · **Tse-Yen Wang[2]** · **Yu-Ta Chen[2]**

Abstract

This study designs and characterizes a novel optical system for simultaneously measuring the thickness (> 1 mm) and refractive index of a transparent plate with two optical paths. The proposed optical system is based on triangulation methods. In contrast to exiting optical system based on triangulation methods for simultaneous measurements of thickness and refractive index of a transparent plate, the proposed optical system can measure a greater thickness with a simpler structure and lower cost. The two optical paths are combined using a self-written measurement processing algorithm to simultaneously calculate the thickness and refractive index. The principle and measurement methodology of the proposed optical system are analyzed and explained. The performance of the proposed optical system is then verified and evaluated experimentally using a laboratory-built prototype. The experimental results show that the measured thicknesses and refractive indexes for Sample B (the thickness > 1 mm) are in good agreement with those determined by a commercial instrument with the maximum deviation of 0.019% for the thickness d and 0.007% for the refractive index n, respectively.

1 Introduction

To characterize the optical and transmission properties of various optically transparent plates and films, their thicknesses and refractive indices are fundamental parameters [1, 2]. For this purpose, the measurement of the thickness and refractive index of transparent materials is very important in various applications [3, 4]. Optical inspection systems are an attractive solution for the inspection process in automated mass production lines due to their high throughput, good reliability, and relatively low cost [5–8]. Because optical inspection systems have long been crucial tools in the non-destructive characterization of materials and devices, they are widely applied for the measurement of these parameters [1, 9]. As a result, various interesting optical methods of addressing this task have been developed in prior art in recent years. Existing measurement methods include the use of dual-confocal microscopy [1], wavelength-scanning interferometry [2, 3], Fabry–Perot interferometry [10], double-slit interferometry [11], Mach–Zehnder interferometry [12, 13], low-coherence interferometry [14–18], optical diffraction tomography [19, 20], optical coherence tomography [21–23], ellipsometry [9, 24, 25], diffractive element [26], triangulation methods [27–29], electronically controlled tunable lens [4], and so forth. In general, the optical methods for simultaneous measurement of the thickness and refractive index of materials are convincing, because they are time saving and robust in the measurement process.

The most common optical methods for simultaneous measurement of the thickness and refractive index of materials can be broadly classified as interferometry, ellipsometry, and triangulation methods. To the best of the authors' knowledge, interferometry and ellipsometry are used to measure thin films and electronic glass (thickness of < 1 mm), and they require complex instrumentation with high resolution and high cost. Therefore, they are not suitable for in-line real-time measurements [2]. In contrast, triangulation

✉ Chien-Sheng Liu
  csliu@mail.ncku.edu.tw

  Tse-Yen Wang
  wangzeyan517@gmail.com

  Yu-Ta Chen
  michael102518@gmail.com

[1] Department of Mechanical Engineering, National Cheng Kung University, No.1, University Road, Tainan 70101, Taiwan, Republic of China

[2] Department of Mechanical Engineering and Advanced Institute of Manufacturing with High-tech Innovations, National Chung Cheng University, No.168, University Road, Minhsiung Township, Chiayi County 62102, Taiwan, Republic of China

methods are particularly attractive for in-line real-time measurements and most popular due to their simpler structures and lower cost. Triangulation methods are widely adopted by laser displacement sensors currently [30, 31]. Triangulation means distance measurement by angle calculation. When using triangulation methods, a light source projects a laser spot onto a measured target. The reflected light falls incident onto a CCD sensor at a certain angle depending on the distance. From the position of the light spot on the CCD sensor and the distance from the sender to the CCD sensor, the distance to the measured target is calculated [32]. However, these techniques based on triangulation methods in prior art are very few and they are difficult to measure a greater thickness (> 1 mm) of transparent plate.

Accordingly, the present study develops a novel optical system based on triangulation methods for simultaneous measurement of the thickness (> 1 mm) and refractive index of a transparent plate. The proposed optical system can measure a transparent plate with thickness of > 1 mm with a simpler structure and lower cost. The proposed optical system is characterized numerically, then verified experimentally using a laboratory-built prototype, and finally compared with a commercial instrument.

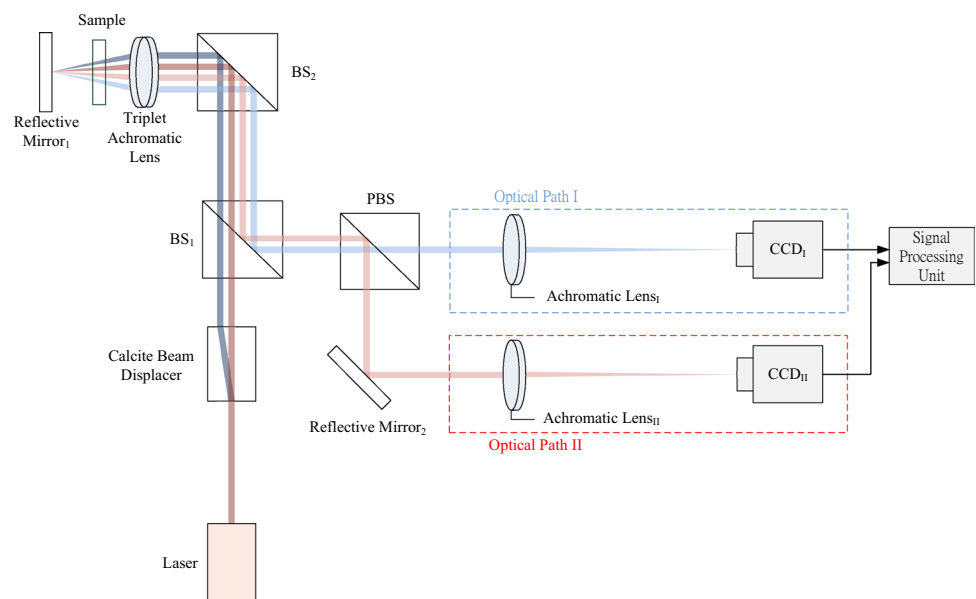## 2 Proposed optical system with two optical paths

2.1 Structure layout

Figure 1 illustrates the structure of the proposed optical system for simultaneously measuring the thickness and refractive index of a transparent plate with two optical paths. As shown, the light beam emitted from a laser light source (Unice, LHRP-0201, 633 nm) passes through a calcite beam displacer (Thorlabs, BD27), where it is split into two separate polar light beams. It is noted that there are many methods for having two parallel beams, for example, using an unpolarized LED light source, a beam splitter (BS), and a reflective mirror to separate one beam into two parallel beams. The two light beams are then passed through two beam splitters (BS1 and BS2, Thorlabs, CM1-BS013), a triplet achromatic lens (Thorlabs, TRS127-020-A), and a transparent sample and are incident on a first reflective mirror surface. The two light beams reflected from the first reflective mirror surface pass back through the sample, the triplet achromatic lens, and two BSs and are then incident on a polar beam splitter (PBS, Edmund, 4SF2-550), where it is split into two separate optical paths. In this study, the triplet achromatic lens is used as an objective lens. In one optical path (designated as Optical Path I), the light beam emerging from the PBS is passed through a first achromatic lens (Thorlabs, AC254-200A) and is then incident on a first CCD sensor (Basler scA1390-17 fm, referred to hereafter as CCD_I). Meanwhile, in the second optical path (designated as Optical Path II), the light beam reflected from the second reflective mirror surface passes through a second achromatic lens (Thorlabs, AC254-200A) and is then incident on a second CCD sensor (Basler scA1390-17 fm, referred to hereafter as CCD_{II}).

In realizing the simultaneous measurement of the thickness and refractive index of the transparent sample, the two optical paths are combined using a self-written measurement processing algorithm to achieve a rapid measuring capability and a high measuring accuracy. We could understand that there are some birefringence and

Fig. 1 Structure of the proposed optical system

polarization problems in many samples. Here these problems could be neglected for our testing samples.

Fig. 2 Schematic illustration of optical paths in the proposed optical system: **a** without sample and **b** with sample

2.2 Measuring principle

Figure 2a, b presents the schematic illustrations of the optical paths within the proposed optical system without and with the transparent sample, respectively. As shown in **a**, when the transparent sample is not put into the proposed optical system (without sample), the light beams in Optical Path I and Optical Path II are finally incident on the center points of CCD_I and CCD_{II}, respectively. However, as shown in **b**, when the transparent sample is put into the proposed optical system (with sample), the light beams in Optical Path I and Optical Path II are finally incident on the off-center points of CCD_I and CCD_{II} with shift distances Δ_I and Δ_{II}, respectively. From basic geometric principles, the following equations for Optical Paths I and II can be obtained, respectively:

$$2z_I = \frac{\Delta_I f_1}{f_{2I}}, \tag{1I}$$

$$2z_{II} = \frac{\Delta_{II} f_1}{f_{2II}}, \tag{1II}$$

where $2z_I$ and $2z_{II}$ are the shift distance of light beam in the triplet achromatic lens, f_1 is the focal length of the triplet achromatic lens, and f_2 is the effective focal length of the achromatic lens.

Figure 3 presents the detailed illustration of optical path I in Fig. 2b. From the triangles ABC and ABD, the following equations can be obtained, respectively:

$$d \tan \theta_I' = y_I, \tag{2}$$

$$d \tan \theta_I = y_I + z_I, \tag{3}$$

where d is the thickness of the sample, θ_I is the incidence angle of Optical Path I, and θ_I' is the refractive angle of Optical Path I. Subtracting Eq. (2) from Eq. (3), d can be obtained as:

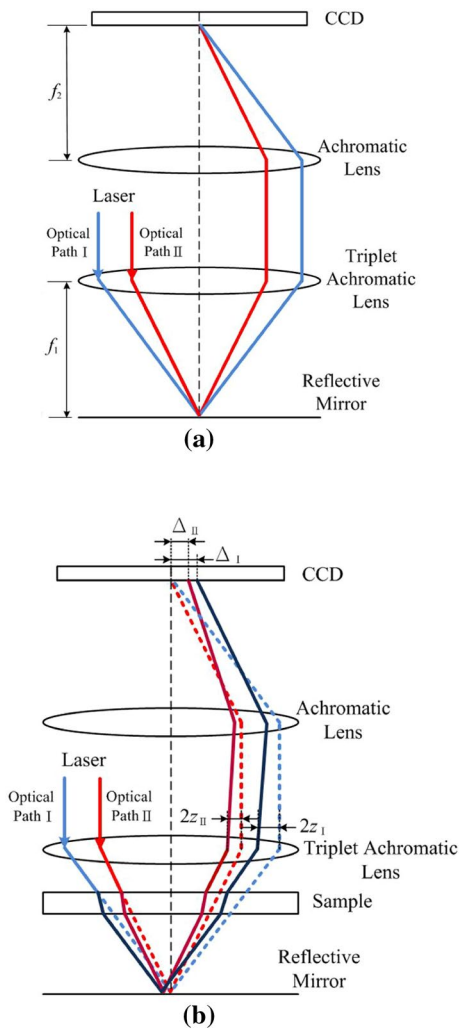$$d = \frac{z_I}{\tan \theta_I - \tan \theta_I'}. \tag{4}$$

Fig. 3 Detailed illustration of Optical Path I in Fig. 2b
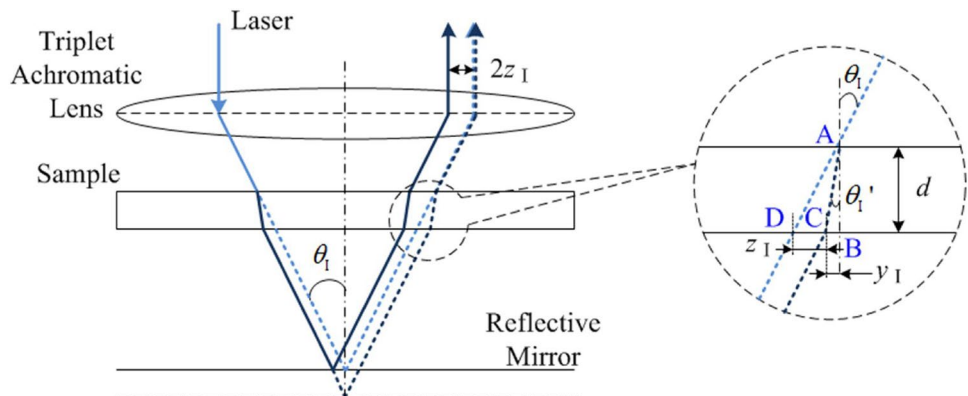
Fig. 4 ZEMAX optical model of the proposed optical system
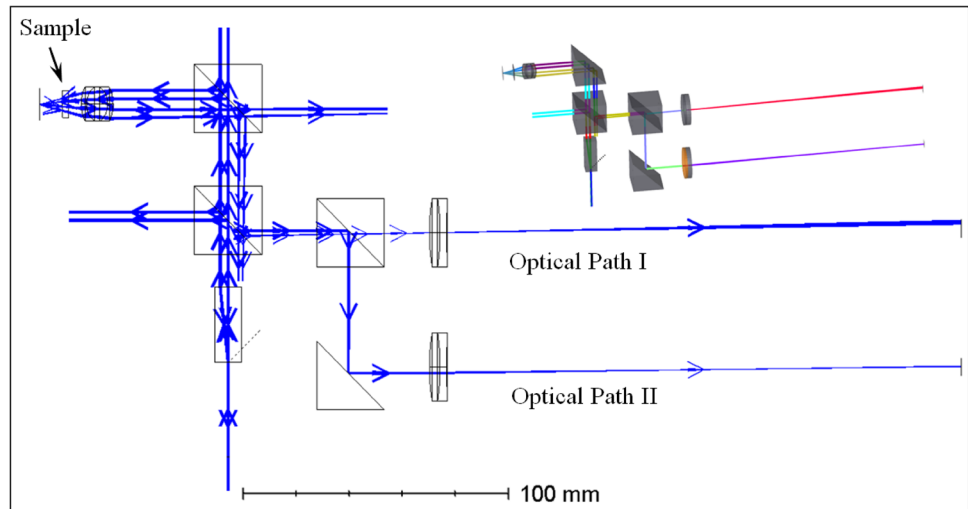
Table 1 Design parameters of the proposed optical system

Variable	Optical Path I	Optical Path II
Laser light source (nm)	633	633
Refractive index of air	1.0	1.0
Focal length of triplet achromatic lens f_1 (mm)	20.4	20.4
Focal length of achromatic lens$_I$ f_{2I} (mm)	200	–
Focal length of achromatic lens$_{II}$ f_{2II} (mm)	–	200
Incidence angle θ_I (°)	14.5602	–
Incidence angle θ_{II} (°)	–	5.6576
CCD$_I$	Basler scA1390-17 fm	–
CCD$_{II}$	–	Basler scA1390-17 fm

In general, the refractive angle θ_I' between two optical media satisfies Snell's law, i,e.,

$$n_0 \sin \theta_I = n \sin \theta_I', \tag{5}$$

where n_0 is the refractive index of air and n is the refractive index of the sample. Equation (5) can be rewritten as

$$\tan \theta_I' = \frac{n_0 \sin \theta_I}{\sqrt{n^2 - n_0{}^2 \sin^2 \theta_I}}. \tag{6}$$

Substituting Eq. (6) into Eq. (4), the following equations for Optical Paths I and II can be obtained, respectively:

$$d = \frac{z_I}{\tan \theta_I - \frac{n_0 \sin \theta_I}{\sqrt{n^2 - n_0{}^2 \sin^2 \theta_I}}}, \tag{7I}$$

$$d = \frac{z_{II}}{\tan \theta_{II} - \frac{n_0 \sin \theta_{II}}{\sqrt{n^2 - n_0{}^2 \sin^2 \theta_{II}}}}. \tag{7II}$$

The measuring principle of the proposed optical system is described by the following. When the transparent sample is measured, the light beams in Optical Path I and Optical Path II are altered, which produce centroid's changes in the positions of the light spots on CCD$_I$ and CCD$_{II}$ with shift distances Δ_I and Δ_{II}, respectively. Here, the off-center shift distances Δ_I and Δ_{II} are obtained by finding the centroids of the images captured by the CCD sensors. From Eq. (1), z_I and z_{II} can be obtained. Then substituting z_I and z_{II} into Eqs. (7I) and (7II), the thickness d and the refractive index n of the sample can be obtained simultaneously. When the sample is measured, the thickness d and the refractive index n will simultaneously alter the laser beams incident on CCD$_I$ and CCD$_{II}$, which in turn induce changes in the positions of the light spots on CCD$_I$ and CCD$_{II}$.

To accurately and efficiently analyze the relation between position information of light spots and the individual thickness d and refractive index n, the laser beam progression in the proposed optical system is tracked using a skew-ray tracing method and a self-written measurement processing algorithm. Light beam tracing equations must be established via a homogeneous transformation matrix (HTM) and skew-ray tracing method proposed by Lin to model and perform ray tracing for the proposed optical system in this study [33–36]. The HTM corresponding to the coordinate frame of each optical
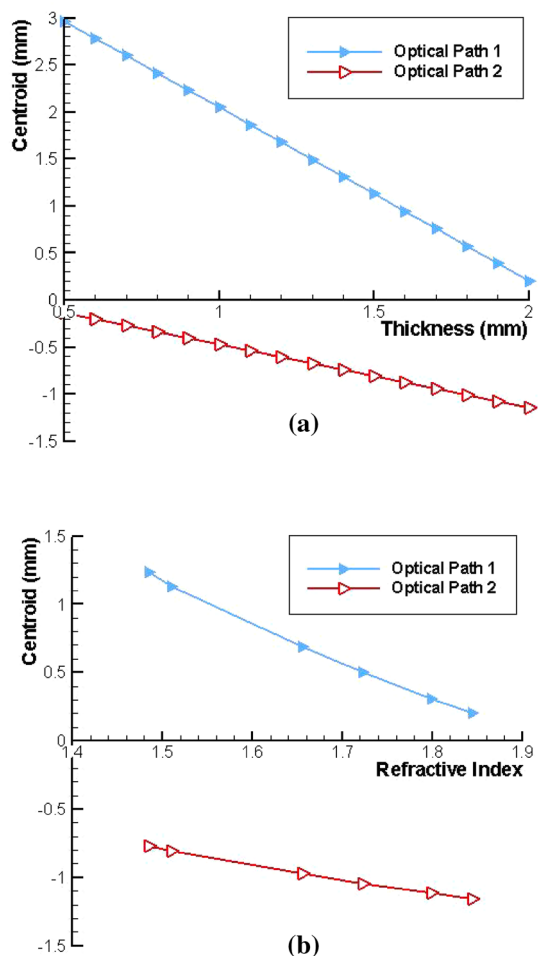
Fig. 5 Simulation results for variation of image centroid position with **a** thickness ($n = 1.515$) and refractive index ($d = 1$ mm)

Fig. 6 Numerical results: **a** variation of calculated thickness with original thickness ($n = 1.515$) and **b** variation of calculated refractive index with original refractive index ($d = 1$ mm)

boundary relative to a reference coordinate system is defined sequentially. A mathematical model is proposed to develop a systematic forward and reverse mathematical derivation. Then, the self-written measurement processing algorithm, which combines the mathematical model and Newton–Raphson method, is used to calculate the individual thickness d and refractive index n of the sample. HTM and the skew-ray tracing method are powerful tools in this field and we only introduce their basic background to avoid repeat in this study. For more comprehensive coverage, the reader is referred to [33–36].

3 Numerical simulation of the proposed optical system

A series of ray tracing simulations were performed to verify the measuring performance of the proposed optical system and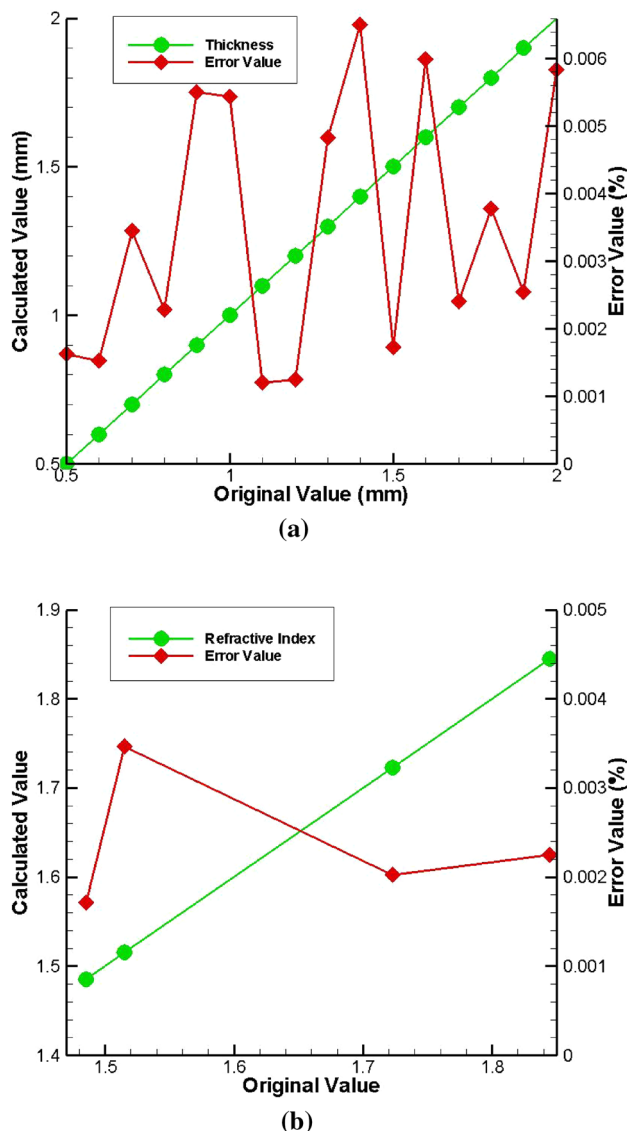 to determine suitable values of the major design parameters. In this section, the ray trace function of ZEMAX software was used to simulate the actual ray propagation in the proposed optical system. The Matlab software was then used to process the images of the laser spot position map and calculate the location of the image centroid. Figure 4 illustrates the detailed optical model constructed using commercial ZEMAX software. Table 1 summarizes the selected values of each design parameter.

Figure 5a, b illustrates the simulation results obtained for the variation of the image centroid with the thickness d (at $n = 1.515$) and refractive index n (at $d = 1$ mm) of the sample in the two optical paths, respectively. These figures indicate that the laser spots on CCD_I and CCD_{II} show a changing trend when the sample experiences a change in thickness d
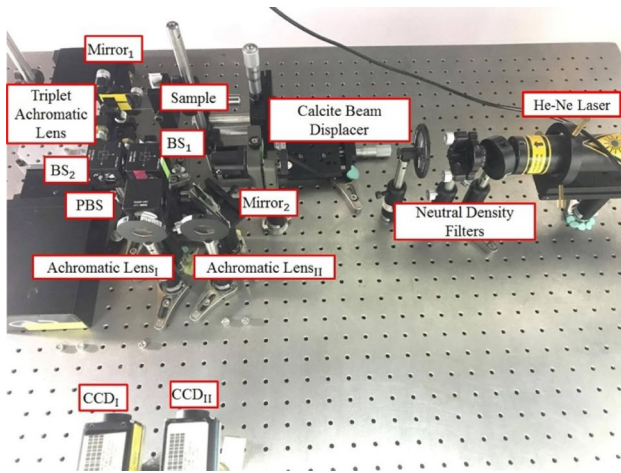
Fig. 7 Laboratory-built prototype of the proposed optical system

or refractive index n. Figures 6a, b presents the numerical results obtained for the thickness d (at $n = 1.515$) and the refractive index n (at $d = 1$ mm), respectively, given different original values, in which the errors of the point to point for the thickness d and refractive index n are plotted, respectively, too. In Fig. 6, the original values of the thickness and refractive index for the samples are the setting values in the ZEMAX model. The calculated values of the thickness and refractive index for the samples are the calculated values using the self-written measurement processing algorithm. Here, the threshold values in Newton–Raphson method are set as 0.007 and 0.005% for the thickness d and the refractive index n, respectively. It is observed that the maximal calculated errors of the thickness d and refractive index n are 0.0065 and 0.0045%, respectively. These calculated errors are very small; in other words, the numerical results are consistent with the theoretical analysis presented in Sect. 2.2.
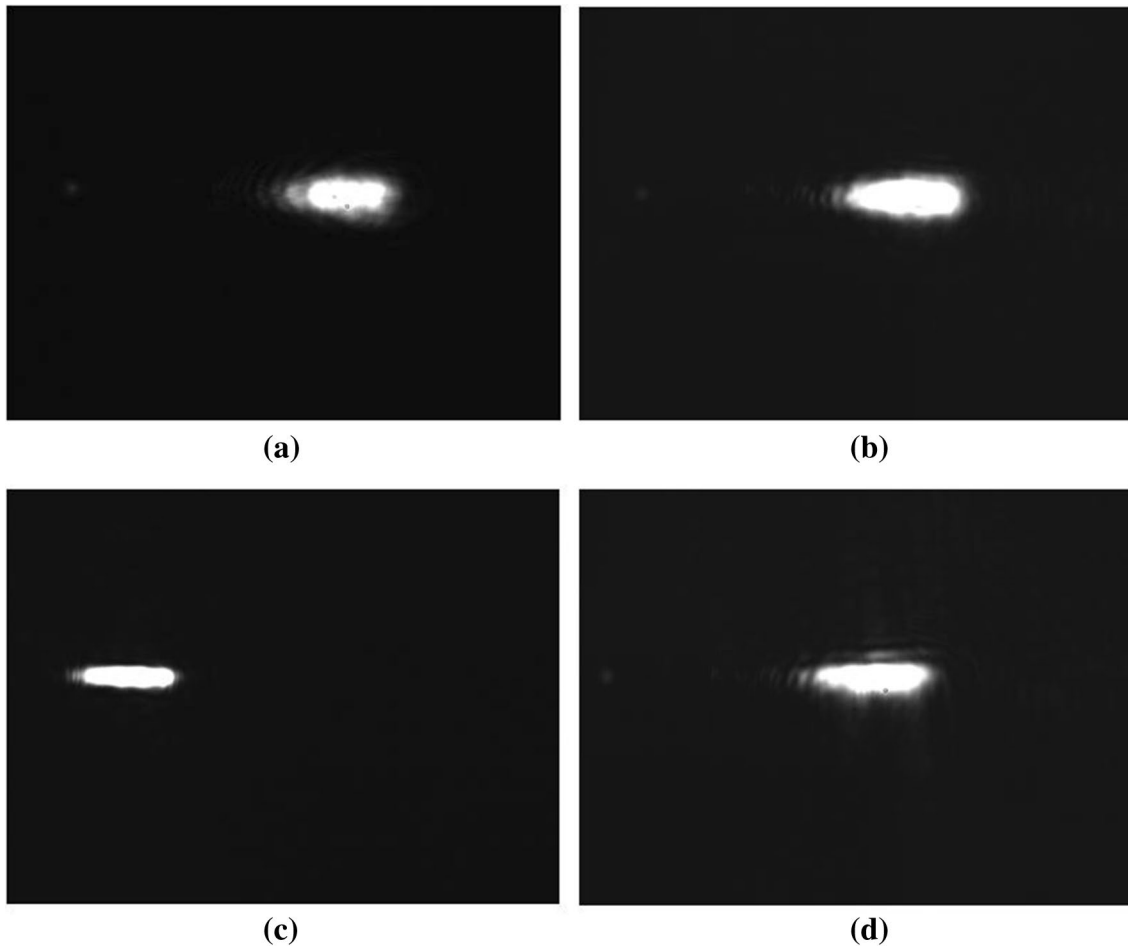

Fig. 8 Captured images of laser spots on CCD$_I$: **a** before inserting sample, **b** after inserting Sample A, **c** after inserting Sample B, and **d** after inserting Sample C
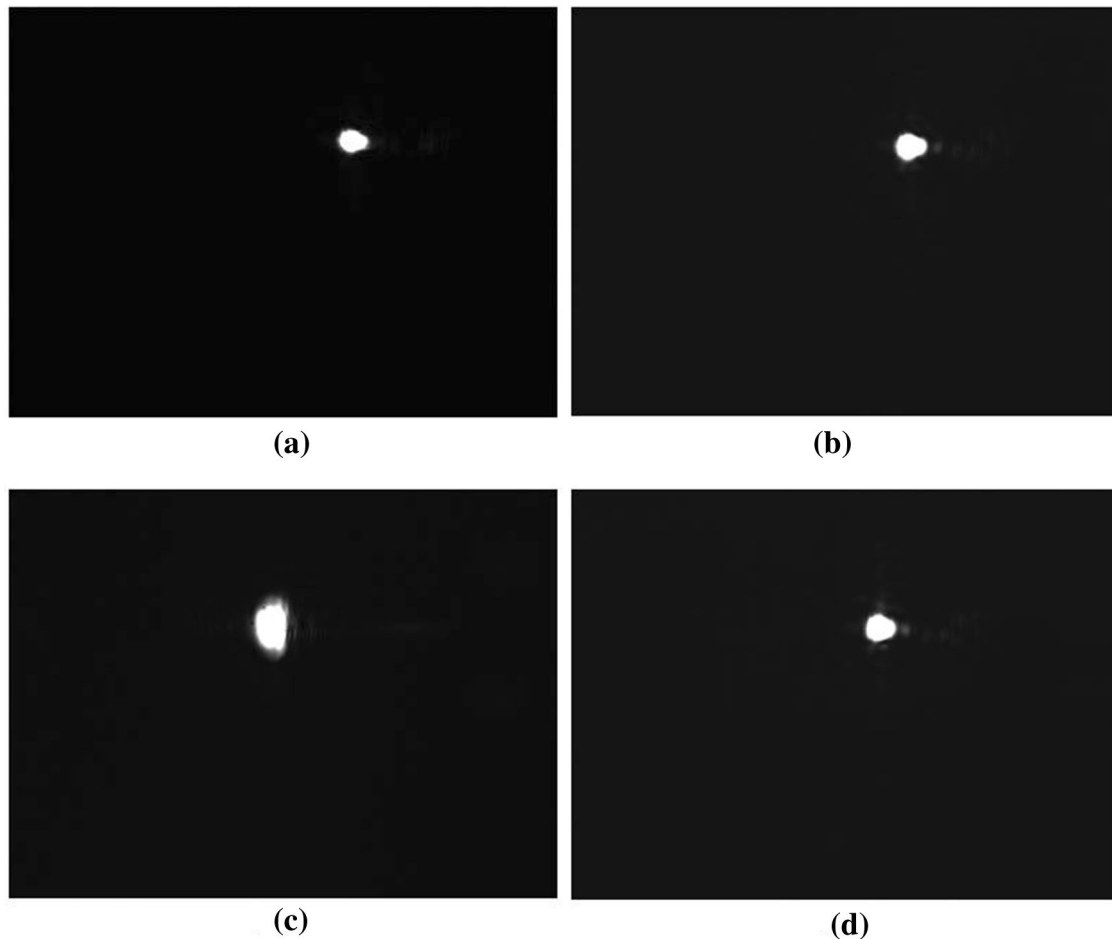
Fig. 9 Captured images of laser spots on CCD_{II}: **a** before inserting sample, **b** after inserting Sample A, **c** after inserting Sample B, and **d** after inserting Sample C

4 Experimental characterization of prototype model

As shown in Fig. 7, the validity of the proposed optical system was verified by means of a laboratory-built prototype with three micro slide samples. The experiments are conducted in a temperature-controlled laboratory and a commercial instrument (Keyence LK-G80 laser displacement sensor) was used to compare and verify the measured accuracy of the proposed optical system. It is noted that Keyence LK-G80 laser displacement sensor cannot simultaneously measure the thickness and refractive index of the sample.

In experimental trials, the thickness d and refractive index n are measured in turn for selected ten points on three samples (Sample A, Sample B, and Sample C) with different thicknesses and refractive indexes. The thickness of Sample B is greater than that of Sample C and the thickness of Sample C is greater than that of Sample A. Figures 8 and 9 present the captured images of the laser spots on CCD_I and

CCD_{II} before and after inserting the three samples, respectively. Figures 10, 11, and 12 present the measured results obtained for the thickness d and refractive index n of Sample A, Sample B, and Sample C, respectively. In these figures, each measured value is the average value of ten repeated experiments on each point to reduce the random errors and the error bar presents the standard deviation on each point. The average standard deviations for the measured thickness d and refractive index n of Sample A, Sample B, and Sample C are listed in Table 2, respectively. It is observed that compared with the measured results of the commercial instrument, the proposed optical system achieves a high measuring accuracy (less than 3 µm for thickness d and 0.003 for refractive index n) with Sample A, in which the measured errors of the thickness d and refractive index n are less than 0.35 and 0.2%, respectively. For Sample C, the proposed optical system achieves a higher measuring accuracy (less than 2.2 µm for thickness d and 0.003 for refractive index n), in which the measured errors of the thickness d and refractive

Fig. 10 Experimental results of Sample A: **a** measured thickness and **b** measured refractive index
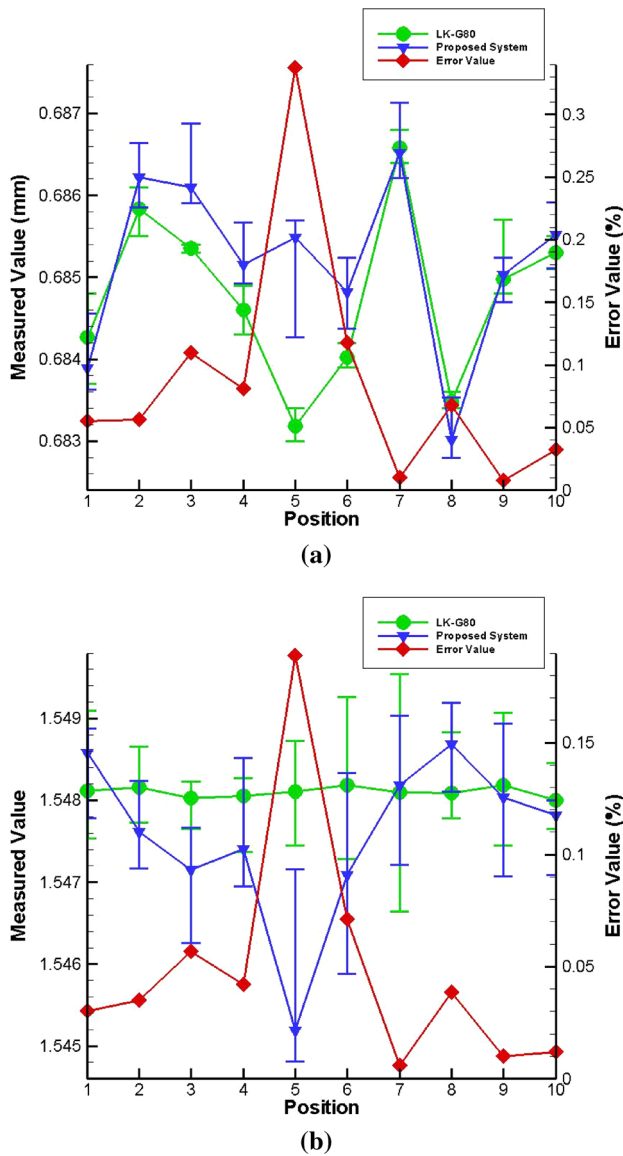
Fig. 11 Experimental results of Sample B: **a** measured thickness and **b** measured refractive index

index n are less than 0.032 and 0.025%, respectively. However, for Sample B, the proposed optical system achieves the highest measuring accuracy (less than 0.4 μm for thickness d and 0.0001 for refractive index n), in which the measured errors of the thickness d and refractive index n are less than 0.019 and 0.007%, respectively. These experimental results are summarized in Table 2 to compare them all together.

From Eqs. (7I) and (7II), z_I and z_{II} increase in proportion to the thickness d of the sample, which means the sensitivity of the proposed optical system is better with a greater thickness of sample. In other words, the signal-to-noise ratio (SNR) of the proposed optical system is greater with a greater thickness of sample. This is why the proposed optical system achieves a higher measuring
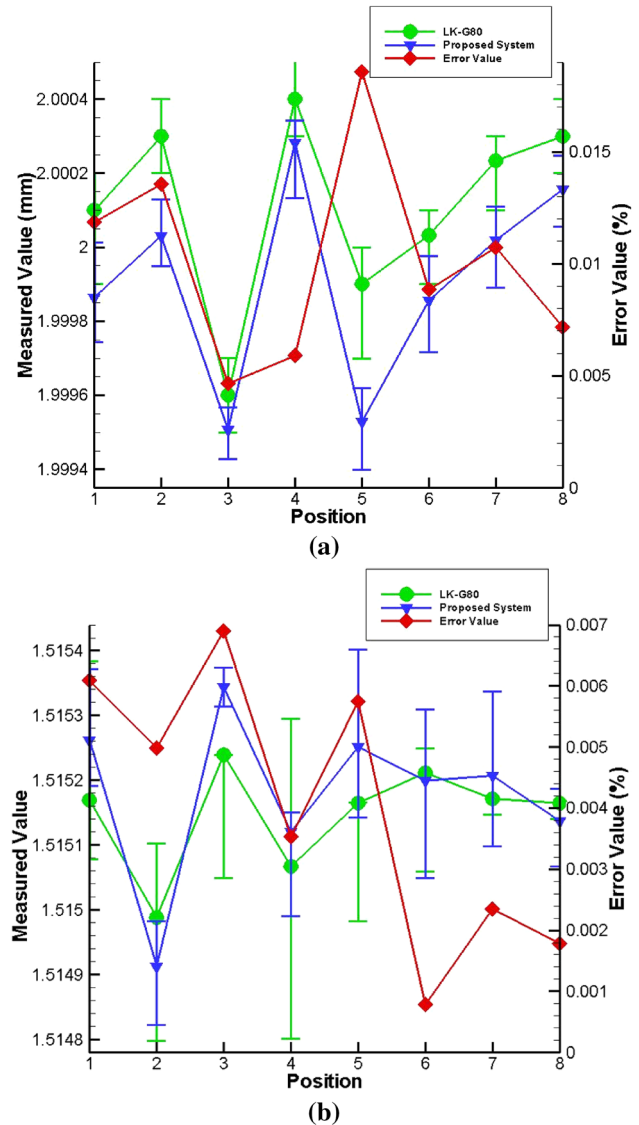
accuracy with a greater thickness of sample. The resulting thicknesses and refractive indices using the proposed optical system are in good agreement with those determined by the commercial instrument. Consequently, it confirms that the proposed optical system is suitable and has potential for simultaneous measurement of the thickness and refractive index of a transparent plate (thickness of > 1 mm) with a simpler structure and lower cost. The proposed optical system is aimed at the specific measurement applications of the car and building windows.

However, the response time of the proposed optical system is less than 47 s now. When compared to commercial products, the proposed system using a laboratory-built prototype spends much time in our measurement process, because we use LabVIEW software and PC to perform

Table 2 Experimental results and comparison of samples

Variable		Proposed system	LK-G80
Simultaneous measurement of thickness and refractive index		Yes	No
Sample A	Standard deviation of measured thickness (μm)	0.9	0.5
	Standard deviation of measured refractive index	0.0016	0.0014
Sample B	Standard deviation of measured thickness (μm)	0.2	0.2
	Standard deviation of measured refractive index	0.0002	0.0004
Sample C	Standard deviation of measured thickness (μm)	0.3	0.3
	Standard deviation of measured refractive index	0.0002	0.0003

the image acquisition and calculate the centroid, and use MATLAB software to calculate the individual thickness d and refractive index n of the sample using a self-written measurement processing algorithm. Therefore, in the future, we will try to organize a new research group, and the proposed system will be combined with a sturdy computer engineering to enable the proposed system for in-line real-time measurement.
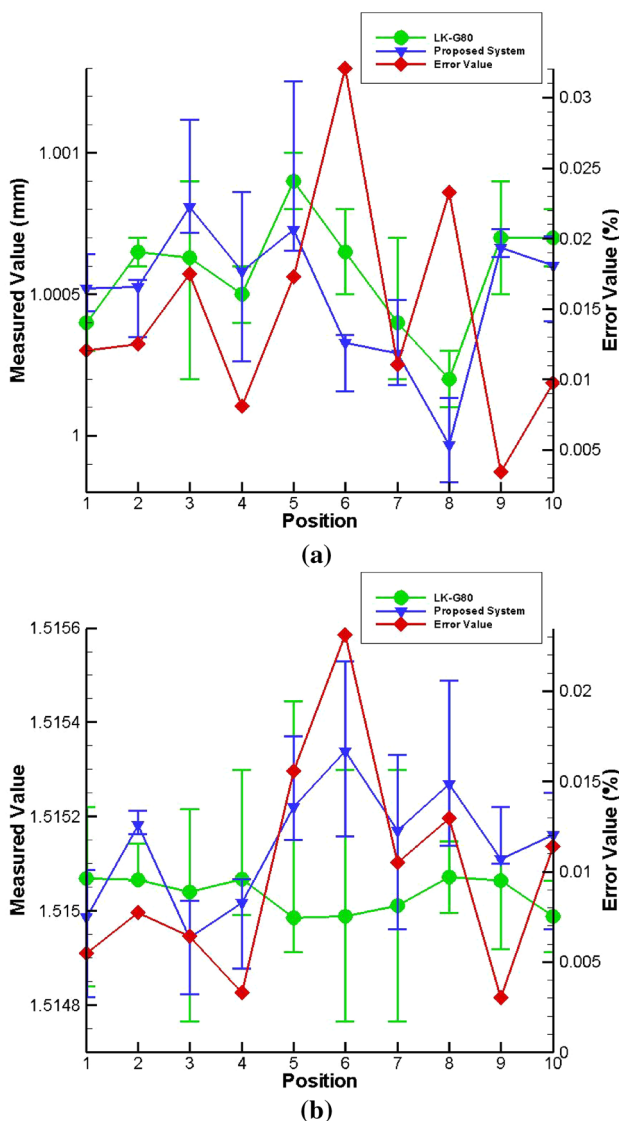
5 Conclusions

This study has presented a novel optical system based on triangulation methods for simultaneous measurement of the thickness (> 1 mm) and refractive index of a transparent plate. The performance of the proposed optical system has been evaluated using a laboratory-built prototype. The experimental results have shown that the optical system has a high measuring accuracy. When compared with the commercial instrument, the measured errors of the thickness d and refractive index n for the proposed optical system are less than 0.019 and 0.007%, respectively, with the transparent plant (Sample B).

Fig. 12 Experimental results of Sample C: **a** measured thickness and **b** measured refractive index

References

1. I.K. Ilev, R.W. Waynant, K.R. Byrnes, J.J. Anders, Dual-confocal fiber-optic method for absolute measurement of refractive index and thickness of optically transparent media. Opt. Lett. **27**(19), 1693–1695 (2002)
2. G. Coppola, P. Ferraro, M. Iodice, S.D. Nicola, Method for measuring the refractive index and the thickness of transparent plates with a lateral-shear, wavelength-scanning interferometer. Appl. Opt. **42**(19), 3882–3887 (2003)
3. T. Fukano, I. Yamaguchi, Separation of measurement of the refractive index and the geometrical thickness by use of a wavelength-scanning interferometer with a confocal microscope. Appl. Opt. **38**(19), 4065–4073 (1999)
4. S.A. Reza, M. Qasim, Nonbulk motion system for simultaneously measuring the refractive index and thickness of a sample using tunable optics and spatial signal processing-based Gaussian beam imaging. Appl. Opt. **55**(2), 368–378 (2016)

5. J.H. Kang, C.B. Lee, J.Y. Joo, S.K. Lee, Phase-locked loop based on machine surface topography measurement using lensed fibers. Appl. Opt. **50**, 460–467 (2011)

6. C.S. Liu, Z.Y. Wang, Y.C. Chang, Design and characterization of high-performance autofocusing microscope with zoom in/out functions. Appl. Phys. B **121**(1), 69–80 (2015)

7. C.S. Liu, S.H. Jiang, Precise autofocusing microscope with rapid response. Opt. Lasers Eng. **66**, 294–300 (2015)

8. C.S. Liu, S.H. Jiang, Design and experimental validation of novel enhanced-performance autofocusing microscope. Appl. Phys. B **117**(4), 1161–1171 (2014)

9. S. Srisuwan, C. Sirisathitkul, S. Danworaphong, Validation of photometric ellipsometry for refractive index and thickness measurements. MAPAN-J. Metrol. Soc. India **30**(1), 31–36 (2015)

10. C. Moreno-Hernández, D. Monzón-Hernández, I. Hernández-Romano, J. Villatoro, Single tapered fiber tip for simultaneous measurements of thickness, refractive index and distance to a sample. Opt. Express **23**(17), 22141–22148 (2015)

11. J.A. Kim, J.W. Kim, T.B. Eom, J. Jin, C.S. Kang, Vibration-insensitive measurement of thickness variation of glass panels using double-slit interferometry. Opt. Express **22**(6), 6486–6494 (2014)

12. J. Park, J. Bae, J. Jin, J.A. Kim, J.W. Kim, Vibration-insensitive measurements of the thickness profile of large glass panels. Opt. Express **23**(26), 32941–32949 (2015)

13. H. Fu, H. Li, M. Shao, N. Zhao, Y. Liu, Y. Li, X. Yan, Q. Liu, TCF-MMF-TCF fiber structure based interferometer for refractive index sensing. Opt. Lasers Eng. **69**, 58–61 (2015)

14. W.V. Sorin, D.F. Gray, Simultaneous thickness and group index measurement using optical low-coherence reflectometry. IEEE Photon. Technol. Lett. **4**(1), 105–107 (1992)

15. J. Na, H.Y. Choi, E.S. Choi, C. Lee, B.H. Lee, Self-referenced spectral interferometry for simultaneous measurements of thickness and refractive index. Appl. Opt. **48**(13), 2461–2467 (2009)

16. S. Kim, J. Na, M.J. Kim, B.H. Lee, Simultaneous measurement of refractive index and thickness by combining low-coherence interferometry and confocal optics. Opt. Express **16**(8), 5516–5526 (2008)

17. P. Balling, P. Mašika, P. Křen, M. Doležal, Length and refractive index measurement by Fourier transform interferometry and frequency comb spectroscopy. Meas. Sci. Technol. **23**(9), 094001 (2012)

18. S.C. Zilio, Simultaneous thickness and group index measurement with a single arm low-coherence interferometer. Opt. Express **22**(22), 27392–27397 (2014)

19. X. Ma, W. Xiao, F. Pan, Reconstruction method for samples with refractive index discontinuities in optical diffraction tomography. Opt. Lasers Eng. **94**, 58–62 (2017)

20. J. Li, Q. Chen, J. Zhang, Z. Zhang, Y. Zhang, C. Zuo, Optical diffraction tomography microscopy with transport of intensity equation using a light-emitting diode array. Opt. Lasers Eng. **95**, 26–34 (2017)

21. H.C. Cheng, Y.C. Liu, Simultaneous measurement of group refractive index and thickness of optical samples using optical coherence tomography. Appl. Opt. **49**(5), 790–797 (2010)

22. H.C. Cheng, C.T. Huang, Measurement of thickness and refractive index of optical samples simultaneously using full-range one-shot frequency-domain optical coherence tomography. Fiber Integrated Opt **34**(3), 145–156 (2015)

23. J. Yao, J. Huang, P. Meemon, M. Ponting, J.P. Rolland, Simultaneous estimation of thickness and refractive index of layered gradient refractive index optics using a hybrid confocal-scan swept-source optical coherence tomography system. Opt. Express **23**(23), 30149–30164 (2015)

24. D. Pristinski, V. Kozlovskaya, S.A. Sukhishvili, Determination of film thickness and refractive index in one measurement of phase-modulated ellipsometry. J. Opt. Soc. Am. A **23**(10), 2639–2644 (2006)

25. M. Mutha, R.P. Schmid, K. Schnitzlein, Ellipsometric study of molecular orientations of thermomyces lanuginosus lipase at the air–water interface by simultaneous determination of refractive index and thickness. Colloid Surf. Biointerfaces **140**, 60–66 (2016)

26. J. Räsänen, K.E. Peiponen, On-line measurement of the thickness and optical quality of float glass with a sensor based on a diffractive element. Appl. Opt. **40**(28), 5034–5039 (2001)

27. C.H. Liu, Z.H. Li, Application of the astigmatic method to the thickness measurement of glass substrates. Appl. Opt. **47**(21), 3968–3972 (2008)

28. C.H. Liu, S.C. Yeh, H.L. Huang, Thickness measurement system for transparent plates using dual digital versatile disc (DVD) pick-ups. Appl. Opt. **49**(4), 637–643 (2010)

29. C.H. Liu, C.C. Liu, W.C. Huang, Application of astigmatic method and Snell's law on the thickness and refractive index measurement of a transparent plate. Microsyst. Technol. **19**(11), 1761–1766 (2013)

30. J. Sun, J. Zhang, Z. Liu, G. Zhang, A vision measurement model of laser displacement sensor and its calibration method. Opt. Lasers Eng. **51**, 1344–1352 (2013)

31. C.S. Liu, S.H. Jiang, A novel laser displacement sensor with improved robustness toward geometrical fluctuations of the laser beam. Meas. Sci. Technol. **24**(1-), 105101 (2013) -105101–8

32. https://www.micro-epsilon.com/

33. P.D. Lin, New Computation Methods for Geometrical Optics (Springer, 2013)

34. C.Y. Tsai, Free-form surface design method for a collimator TIR lens. J. Opt. Soc. Am. A-Opt. Image Sci. Vis. **33**(4), 785–792 (2016)

35. Y.T. Chen, W.C. Lin, C.S. Liu, Design and experimental verification of novel six-degree-of freedom geometric error measurement system for linear stage. Opt. Lasers Eng. **92**, 94–104 (2017)

36. Y.T. Chen, Y.S. Huang, C.S. Liu, An optical sensor for measuring the position and slanting direction of flat surfaces, Sensors 16(7), 1061-1–1061-13 (2016)